Glass–Ceramic Sealants for Solid Oxide Cells Research at Politecnico di Torino: An Overview on Design, Sinter-Crystallization, Integration and Interfacial Issues

Antonio G. Sabato, Hassan Javed, Milena Salvo, Andreas Chrysanthou, and Federico Smeacetto

Abstract Solid oxide cells (SOCs) devices are of great interest for effective power generation and for highly efficient conversion of electricity to hydrogen, fuels and chemicals using high temperature electrolysis. Electrochemical energy conversion in SOCs can be achieved only by a reliable integration and joining technology. In this context, glass-based materials, with multiple functional compositions and properties play a key role in the performance and durability. In most SOC stack designs the metallic interconnect must be sealed both to the interconnect frame and to other cell ceramics components, thus presenting significant challenges. An overview and update about the research activity done at Politecnico di Torino (Italy) on design, sinter-crystallization, characterization and testing of glasses and glass–ceramics sealants is presented and discussed.

Keywords Glass · Glass–ceramics · Sintering · Crystallization · Solid oxide cells · Sealants

A. G. Sabato
Institut de Recerca en Energia de Catalunya (IREC), Jardins de les Dones de Negre 1, 2ª pl, 08930 Sant Adrià de Besòs, Barcelona, Spain
e-mail: gsabato@irec.cat

H. Javed
Sunfire GmbH, Gasanstaltstraße 2, 01237 Dresden, Germany
e-mail: Hassan.Javed@sunfire.de

M. Salvo · F. Smeacetto (✉)
Department of Applied Science and Technology, Politecnico di Torino, Corso Duca degli Abruzzi 24, 10129 Torino, Italy
e-mail: federico.smeacetto@polito.it

M. Salvo
e-mail: milena.salvo@polito.it

A. Chrysanthou
School of Physics, Engineering and Computer Science, University of Hertfordshire, College Lane, Hatfield AL10 9AB, Hertfordshire, UK
e-mail: a.chrysanthou@herts.ac.uk

F. Baino et al. (eds.), *Ceramics, Glass and Glass-Ceramics*, PoliTO Springer Series,
https://doi.org/10.1007/978-3-030-85776-9_6

1 Glass–Ceramic Sealants for Solid Oxide Cells (SOC) Applications

Glass and glass–ceramics play a fundamental role in the development of SOC technology. Indeed, thanks to their nature, glasses and glass–ceramics can be used as sealants in harsh conditions ensuring a very high gas tightness (leak rate < 10^{-9} mbar l s^{-1}). The use of glass to metal sealing technology is well known in different applications such as hermetic interconnectors, incandescent light bulb, glass-encapsulate diodes, pressure tight glass windows etc. [1, 2].

In SOC technology different materials need to be joined together for use in severe operating conditions. In order to obtain useful SOC performance, it is necessary to combine more cells in a stack connected by an interconnect which is typically made by high Cr-containing stainless steel (the most common being Crofer22APU), while ceramic materials are used for both the electrodes and the electrolyte. Furthermore, SOC stacks operate at high temperatures (700–900 °C) and are exposed to dual atmospheres (reducing and oxidizing) for long periods of time and their lifetime is expected to exceed 40 kh.

The use of sealants is necessary in these systems to ensure the separation between the atmospheres, otherwise their mixing, even due to micro leaks, can lead to fast reduction of the device efficiency as well as to side reactions that may damage the device itself (i.e. formation of hotspots due to strong exothermic reactions). In this scenario, the need for sealants that are able to withstand the high operating temperatures and thermal cycles as well as the aggressive atmospheres has emerged. In recent years, researchers have focused on different sealing approaches; these include the use of a variety of possible sealants including compressive sealants such as mica-based sealants [3–6], metallic-based sealants or rigid ones (like brazes or glass–ceramics). Out of these options, glass–ceramic sealants have been observed to be among the best-performing. The great advantage of the use of these materials as sealants is represented by the possibility of tuning their properties by tailoring their composition. It is possible to change the type or the amounts of the oxides contained in a parent glass in order to obtain favourable properties for the performance of the final glass–ceramic sealant. Properties that can be altered by variation in the glass–ceramic composition include the glass transition temperature, T_g, the softening temperature, T_s, the crystallization temperature, T_c, the crystalline phases and crystallization behaviour, the thermal expansion coefficient (CTE) which is fundamental in SOC applications due to the high operating temperatures as well as its chemical compatibility with the other materials involved in a SOC stack.

In such a challenging application, different factors need to be considered at the same time; a good sealant should not develop detrimental phases with the joined materials at the operating T and should withstand exposure to both oxidizing and reducing atmospheres and of course it must not degrade under these conditions. Furthermore, it has to show excellent thermo-mechanical compatibility with such materials and high electrical resistivity (> 10^4 Ω cm) in order to avoid current losses or short circuits [3–5]. Therefore, it is clear that the starting composition of a glass-based

sealant has to be carefully tailored since an improvement on one of these factors may be concomitant with a worsening of other properties. The development of a suitable glass-based sealant during recent years has attracted the efforts of many players in the scientific community including: Pacific Northwest National Laboratories (PNNL) [7], Denmark Technical University (DTU) [8]. Furthermore, different compositions have been commercialized by SCHOTT and other companies [9].

There is a growing body of literature that recognizes the important and crucial role of sealants. Among these, a strong contribution in the last 10 years has come from Politecnico di Torino and its partners focusing the efforts on production, characterization and testing in real operating conditions of different glass compositions (either containing or in the absence of alkali oxides). In this section, their main results will be summarized.

1.1 Alkali-Containing Glass–Ceramic Sealants at POLITO

Part of the research activity at POLITO on glass–ceramic sealants focused on alkali-containing compositions. The work has addressed topics including their thermal characterization by means of differential thermal analyses (DTA), heating stage microscopy (HSM) and dilatometry (DIL) and their compatibility with typical materials involved in the joining of SOC stacks components including YSZ (electrolyte), Crofer22APU and AISI 441 stainless steels (both bare and coated with different protective coatings).

The introduction of alkali oxides in the glass composition can help the tuning of the CTE of the sealant after its sinter-crystallization, achieving a high thermomechanical compatibility with the sealed materials which typically have a CTE that ranges between 10×10^{-6} and 12×10^{-6} K^{-1}. Furthermore, thanks to their role as network modifiers in a glass, alkali oxides can contribute to the lowering of the characteristic temperatures of the material.

In the case of SOC applications, it is very important to understand the behaviour of a sealant not only in its starting glassy form but especially as a glass–ceramic obtained as a consequence of a sinter crystallization thermal treatment (carried out in order to consolidate the joining process). Indeed, the formation of crystalline phases can strongly influence the overall properties of the material and therefore the soundness of the joining as well as its compatibility in relevant operating conditions.

For this reason, Smeacetto and co-workers [10–13] carried out a variety of studies on the crystallization behaviour of different glasses by DTA measurements demonstrating how these systems tend to crystallize mainly by following a heterogeneous crystallization mechanism, starting from the surface of the glassy particles. It is possible to evaluate the crystallization behaviour of a glass by carrying out DTA measurements on a fixed particle size with different heating rates. Furthermore, DTA analyses on different glass particle sizes may provide understanding of the main crystallization behaviour. Indeed, if heterogeneous crystallization from the surface is the predominant mechanism, a finer powder will give a DTA thermogram with a more

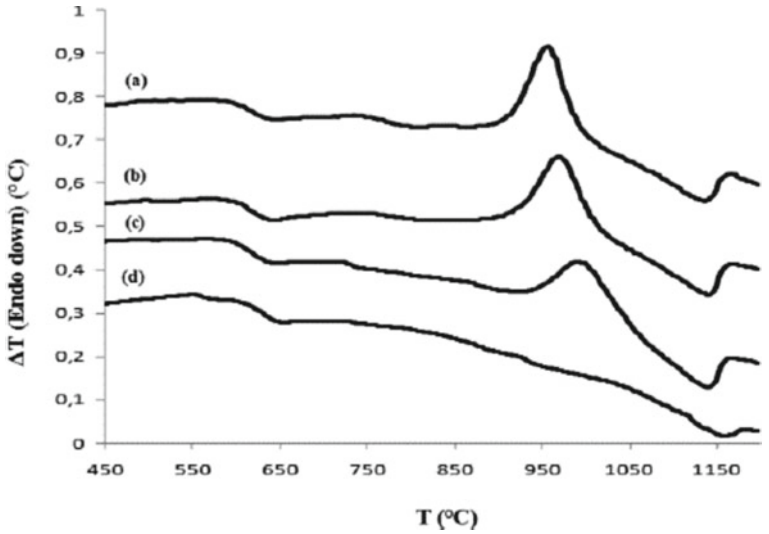

Fig. 1 DTA analyses carried out on alkali-containing glass with different powders dimension at the same heating rate (20 °C/min): **a** < 38 μm, **b** 38–75 μm, **c** > 75 μm, **d** bulk glass [12]

pronounced crystallization peak, in comparison with coarser powders (Fig. 1). A deep understanding of the crystallization mechanism and of the effect of the particle size is fundamental since it can affect the compatibility of a sealant with the interface material. An excessive surface crystallization can lead to high degree of shrinkage with consequent poor wetting on the substrate (as shown in the left image of Fig. 2).

Furthermore, the control of the amount of crystalline phases is also crucial. A certain degree of crystallization can be beneficial for a sealant since the crystalline phase improves the mechanical behaviour of the joint avoiding excessive flowing behaviour of the glass–ceramic at the operating conditions of a SOC stack (much higher of the typical glass transition temperatures). By contrast, a sufficiently residual glassy phase is able to accommodate thermal stresses during the operation at high T. Furthermore, the evolution of the crystalline phases needs to be taken into account since the long-term exposure of these materials $T > T_g$ can lead to changes in the amount and number of crystallized phases in comparison with the "as-joined" state.

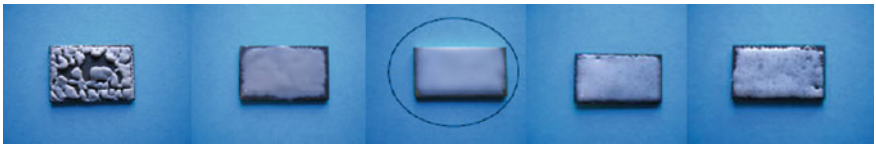

Fig. 2 Effect of different powder sizes on the compatibility between a glass–ceramic sealant (SACN) and a Crofer22APU stainless steel substrate. From left to right different SACN powders sizes: d < 20 μm, d = 20–38 μm, d = 38–75 μm, d = 75–106 μm and d > 106 μm [10]

An example is reported in Figs. 3 and 4 concerning an alkali-containing glass–ceramic labelled as V10. This material was studied after different steps of exposure at 800 °C in static air (100 and 300 h) and its microstructure compared with of its structure after the joining treatment (850 °C for 1 h in air). The XRD analysis (Fig. 3) revealed the formation of Al-containing diopside (with a CTE 11.6 × 10^{-6} K^{-1}) as the only crystalline phase after the joining treatment (≈ 37 wt%) (Fig. 4b). This led to a beneficial increase in the CTE of the sealant from 7.6 × 10^{-6} K^{-1} (parent glass) to 11.5 × 10^{-6} K^{-1} (glass–ceramic), a value that was closer to those of the materials typically involved in a stack. In this case the further aging at 800 °C led to the formation of nepheline (CTE 9 × 10^{-6} K^{-1}) as a secondary crystalline phase (≈8 wt%). The formation of this phase did not affect excessively the CTE of the glass–ceramic and led to a more rigid structure "delaying" the dilatometric softening point (Fig. 4a); the amount of the residual glassy phase was found to be about 50 wt%. This example demonstrates the importance of having knowledge of the evolution of a glass–ceramic sealant for SOC applications, especially when considering the long-term operations expected for these devices.

One of the first alkali-containing glass–ceramic compositions studied at POLITO was labelled SACN (already cited in Fig. 2). This system was extensively studied and exhibited excellent behaviour in terms of compatibility with both YSZ and Crofer22APU. Figure 5 shows the morphology of a YSZ/SACN/Crofer22APU sample in the "as-joined" state, as well as after aging for 400 h in air at 800 °C. Both the SEM pictures revealed good adherence with no evidence of cracks or delamination and there were no adverse reactions even after aging.

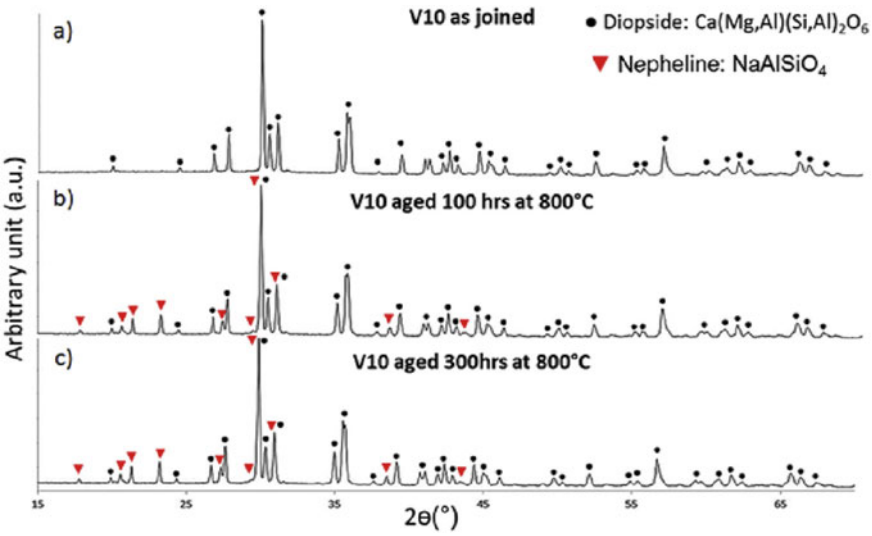

Fig. 3 XRD of V10 glass–ceramic after different aging at 800 °C in air [14]

a)

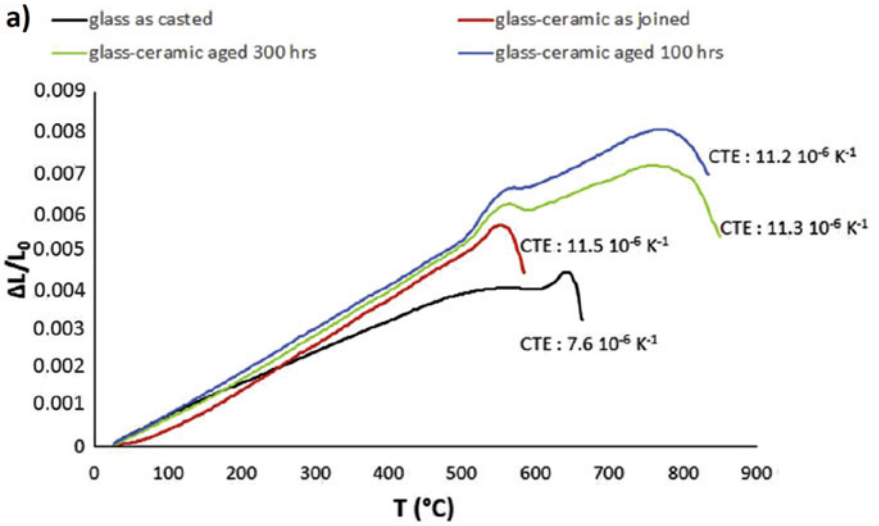

b)

Wt%	Amorphous	Diopside $Ca(Mg,Al)(Si,Al)_2O_6$	Nepheline $NaAlSiO_4$
As-joined	63	37	–
Aged 100 h	49	43	8
Aged 300 h	50	42	8

Fig. 4 Dilatometric measurements of V10 glass as casted and glass–ceramic after different aging at 800 °C in air (**a**) and results of Rietveld quantitative analyses based on XRD reported in Fig. 3 [14]

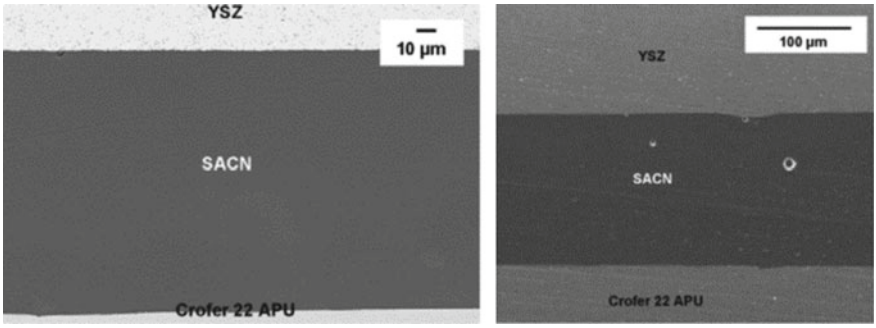

Fig. 5 SEM pictures of a joining Crofer22APU/SACN/YSZ after the joining treatment and after an aging of 400 h at 800 °C [10]

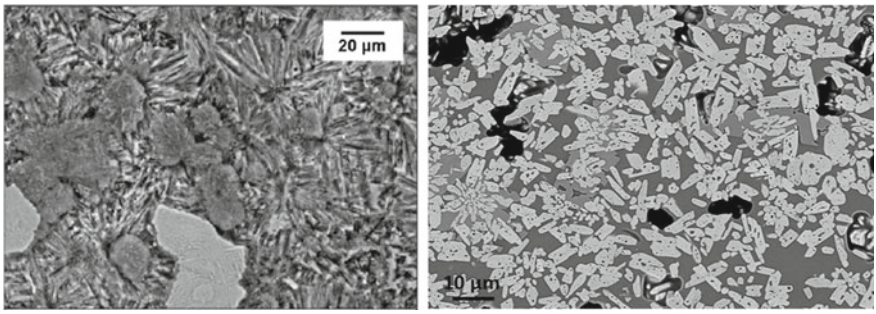

Fig. 6 Comparison between microstructure of a refractory sealant on the left Smeacetto et al. [10] and a compliant one on the right

However, the SACN glass–ceramic showed high crystallinity after the sinter-crystallization treatment. For this reason, the studies that followed focused on glassy systems that were more "compliant" and able to maintain a considerable amount of the residual amorphous phase thanks to a meticulous tailoring of the alkali content. A higher amount of residual glassy phase can be beneficial in real operating conditions ensuring a less rigid behaviour able to accommodate thermal stresses. Furthermore, the amorphous portion could provide self-healing during the thermal cycles. One example was represented by the V10 glass–ceramic. As reported in Fig. 4b after long aging at 800 °C, the residual glassy phase represents ≈ 50 wt% of the material. Figure 6 depicts a clear difference in the microstructure between the refractory glass–ceramic (SACN) and the compliant one (V10).

The behaviour of alkali-containing glasses has been the subject of several research investigations. Some investigations have shown that these glasses can exhibit satisfactory long-term behaviour when tested under harsh conditions [15–23]. There have also been studies in which there was evidence of reaction with Cr leading to formation of Cr-containing volatile species with consequent degradation of the sealant integrity and possible formation of conductive phases which may cause unwanted short circuits.

Sabato et al. [14] carried out an extensive study on the degradation phenomena of an alkali-containing glass–ceramic exposed to real-operating conditions under a dual atmosphere at 800 °C with application of a DC electrical voltage. The electrical resistivity was measured for the duration of the test. The work involved investigation of the behaviour of (i) the glass–ceramic itself with a 1.3 V applied voltage, (ii) a joined sample Crofer22APU/glass–ceramic/Crofer22APU with a 0.7 V applied voltage and (iii) a joined sample Crofer22APU/glass–ceramic/Crofer22APU with a 1.3 V applied voltage. The resulting resistivity measurements are shown in Fig. 7. While in the case of the first two samples the electrical resistivity was found to be stable exhibiting a value of above 10^4 Ω cm for the entire duration of the test, in the case of the sealant interfaced with the metallic counterpart under a higher voltage, fast degradation of the electrical resistivity was recorded.

A detailed post-mortem analysis was carried out on the degraded sample (Fig. 8)

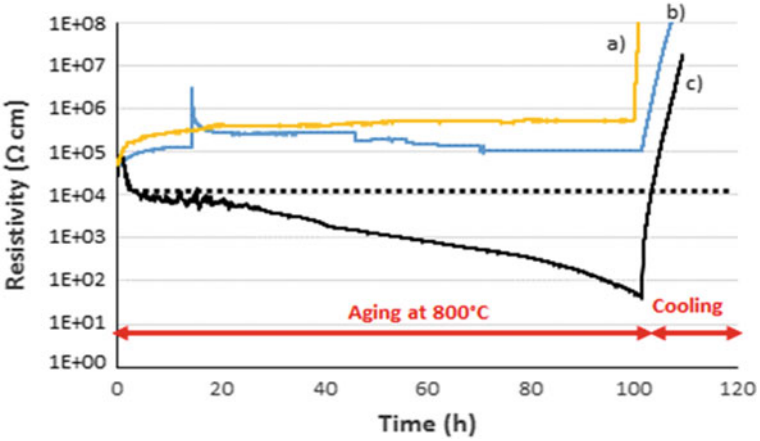

Fig. 7 Electrical resistivity measurements at 800 °C for 100 h of: **a** the glass–ceramic itself at 1.3 V, **b** joined sample Crofer22APU/glass–ceramic/Crofer22APU at 0.7 V and **c** joined sample Crofer22APU/glass–ceramic/Crofer22APU at 1.3 V [14]

showing the development of degradation phenomena at the air side of the sample. The integrity of the sealants seemed to be compromised close to its boundary with the air. Furthermore, the formation of a Cr_2O_3 bridge was detected starting from the cathodic (negative) polarized interface and growing towards the anodic (positive) polarized one. The good electronic conductivity of chromia explained the rapid decrease in the electrical resistivity of the system as reported in Fig. 7. On the other hand, the same phenomenon was not detected when a 0.7 V DC voltage was applied. This behaviour was explained starting with the well-known tendency of Cr-forming alloys to form Cr-containing volatile species in typical SOC operating conditions by the following the reaction:

$$Cr_2O_{3(s)} + 2H_2O_{(g)} + 3/2O_{2(g)} \leftrightarrow 2CrO_2(OH)_{2(g)} \quad (1)$$

$CrO_2(OH)_2$ then reacted with Na contained in the glass forming Na_2CrO_4 which is highly volatile at 800 °C and has a partial pressure much higher than $CrO_2(OH)_2$:

$$CrO_2(OH)_{2(g)} + Na_2O_{(s)} \leftrightarrow Na_2CrO_{4(g)} + H_2O_{(g)} \quad (2)$$

Na_2CrO_4 is reduced at the negative polarized interface forming again Cr_2O_3 under the electrochemical potential applied to this side of the sample:

$$2Na_2CrO_{4(g)} + 2H_2O_{(g)} \rightarrow Cr_2O_{3(s)} + 3/2\ O_2 + 4NaOH_{(g)} \quad (3)$$

Taking into account the fact that reaction 3 has a nominal Nerst potential of 1.19 V at 800 °C, it is clear how this degradation mechanism was triggered at an applied

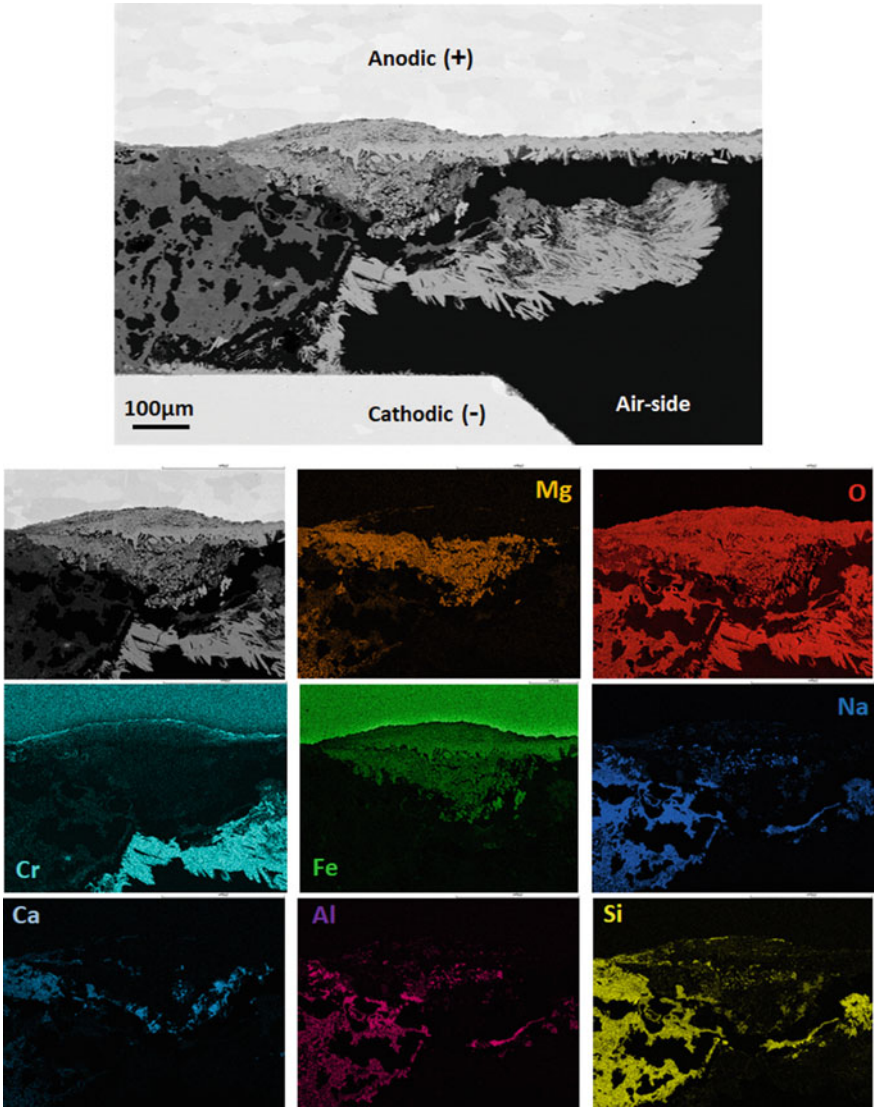

Fig. 8 SEM and EDS elemental mapping of alkali-containing glass–ceramic sealant interfaced with pre-oxidised (900 °C Crofer22APU in a sandwiched sample tested in dual atm. at 800 °C for 100 h under the application of a DC voltage of 1.3 V) [14]

voltage of 1.3 V, but did not take place in the case of the voltage of 0.7 V. Furthermore, the huge Cr reservoir represented by the steel and the re-formation of NaOH as a reaction product of Eq. 3 can lead to continuous catastrophic degradation of these materials under these conditions.

Considering this, despite the use of alkali-containing glasses can bring several advantages from the point of view of thermo-mechanical compatibility at the sealing temperature, a protective layer should be applied when using alkali-containing glass–ceramics.

Another important factor that emerged in the last few years for the successful development and operation of SOCs is the compatibility of glass-based sealants and protective coatings typically used to protect the metallic materials in a SOC stack. Furthermore, the deposition of protective coating can also prevent the development of detrimental reaction between the steels and the glass–ceramic sealants. The most common materials used as protective coatings in this application are represented by the family of spinels based on $(MnCo)_3O_4$ and their variants [24–26]. However, many studies focused also on the use of Al_2O_3 as a protective coating [27–29]. Therefore, the compatibility of the glass-based sealants interfaced with these layers is crucial, especially in the case of design where such contacts are foreseen [15–27, 27, 30, 31].

Good compatibility between the sealants and the protective coatings represents a strong advantage in industrial production allowing the formation of a uniform coating on the entire surface of interconnects without using masking techniques. Furthermore, the presence of a protective coating would block the development of detrimental reactions that may develop between the sealant and bare Cr-containing stainless steels. An example is reported in Fig. 9 that presents SEM and EDS analyses at the interface between a $Mn_{1.5}Co_{1.5}O_4$ coating obtained by electrophoretic deposition and an alkali-containing glass–ceramic sealant. The interface between the coating and the sealant and the underlying steel is in both cases excellent with no evidence of cracks or delamination. The EDS analyses have also shown excellent Cr-retention ability of the coating and the absence of any reaction between the protective layer and the sealant.

Another type of coating often applied to metallic interconnects is represented by a thin layer of alumina that acts as both a barrier layer to prevent Cr evaporation and as a barrier between the sealants and the underlying steel preventing detrimental interaction between the two. Ritucci et al. [27] successfully reported the interfacing of an alkali containing glass–ceramic sealants labelled V11 and alumina-coated Crofer22APU (see Fig. 10). The glass–ceramic appears to have excellent compatibility with the Al_2O_3 layer; the interface is free from cracks and reaction products. The EDS in Fig. 10 also shows that there were no inter-diffusion phenomena. The Cr appears to be confined to the metallic side of the sample.

1.2 Sr-Containing Glass–Ceramic Seals

As discussed in the previous section, alkali and alkaline earth oxides are commonly used as modifiers in glasses; however, alkali metal oxides have the disadvantage of having a high chemical reactivity and low electrical resistivity when in contact with metallic interconnects under applied voltage [32]. In spite of that, a large part of the research on glass–ceramic sealants has focused on the use of BaO as the

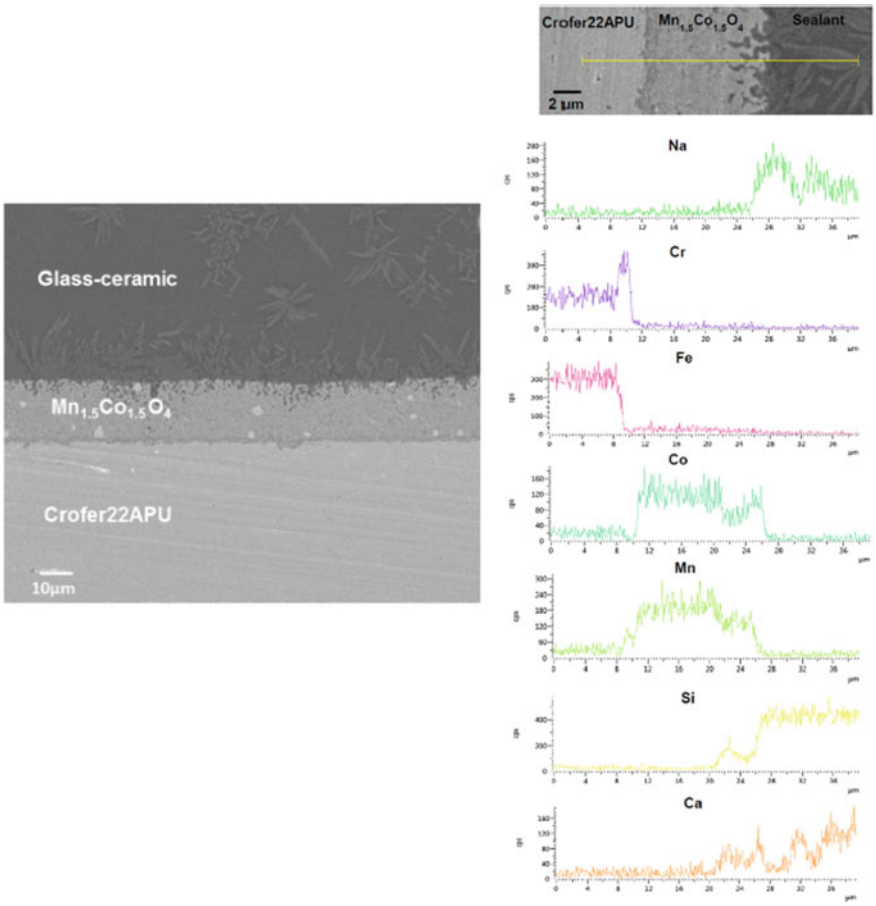

Fig. 9 SEM cross-section of Crofer22APU/protective coating/glass–ceramic sealant after the joining thermal treatment, together with EDS line-scan analyses carried out at the interface between the three materials. $Mn_{1.5}Co_{1.5}O_4$ coating was applied by electrophoretic deposition [17]

main modifier [5, 33–36], while in more recent years, the trend seems to be shifted towards the use SrO [37–44]. Similar to the behaviour of BaO, the addition of SrO also reduces viscosity and adjusts the CTE, but SrO is less prone to form chromates in comparison to BaO. While several studies have assessed the efficacy of SrO-based glasses [40, 42–46], the long-term durability of SrO-containing glasses under SOFC/SOEC conditions is still unclear. Another topic of interest is the fact that the addition of small concentrations of components like B_2O_3, Y_2O_3, Al_2O_3, etc. has been shown to improve the wettability of glasses and adjust the CTE and to control the crystallization behaviour [6, 47].

At POLITO, an extensive research has been conducted to investigate the use of Sr-containing glasses for SOC applications. One of the most promising glass

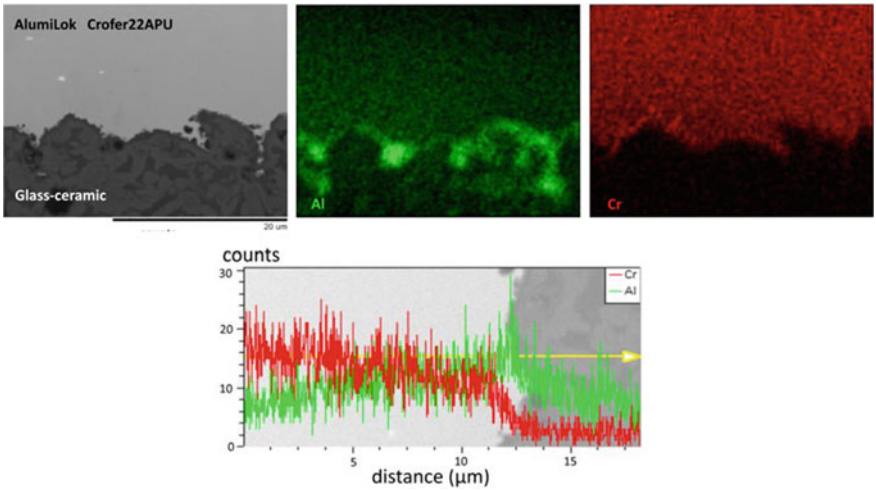

Fig. 10 SEM cross-section and EDS maps and line-scan of interface aluminized Crofer22APU/glass–ceramic sealant as-joined [27]

Table 1 Glass composition of HJ4 glass in mol% [48]

mol%	SiO_2	B_2O_3	SrO	Al_2O_3	Y_2O_3
HJ4	57.6	5.65	28.84	6.17	1.74

compositions that has been developed by the POLITO group is termed as HJ4 glass and the corresponding composition is given in Table 1.

In a SiO_2–SrO based system, a SiO_2/SrO of 1 is required in order to obtain the high CTE $SrSiO_3$ phase (10.9×10^{-6} K^{-1}). However, for SOC sealant applications a high amount of SrO increases the possibility of formation of the unwanted high CTE $SrCrO_4$ phase ($18–20 \times 10^{-6}$ K^{-1}). Therefore, the SiO_2/SrO ratio in the HJ4 glass system was kept to ~ 2 with an aim to minimize the possibility of $SrCrO_4$ formation. On the other hand, the high silica content would also be beneficial considering the high-operating temperatures of the SOECs of 850 °C.

1.2.1 Thermal and Microstructural Analysis

The thermal properties glass transition temperature (T_g), crystallization temperature (T_p) and sintering temperatures of as-cast glass were analysed by differential thermal analysis (DTA) and heating stage microscopy (HSM). The corresponding DTA analysis and the shrinkage behaviour vs temperature, found from HSM, are shown in Fig. 11.

The results have shown that there was no sharp exothermic crystallization peak, thus indicating that the crystallization in HJ4 glass was not sufficient to be identified

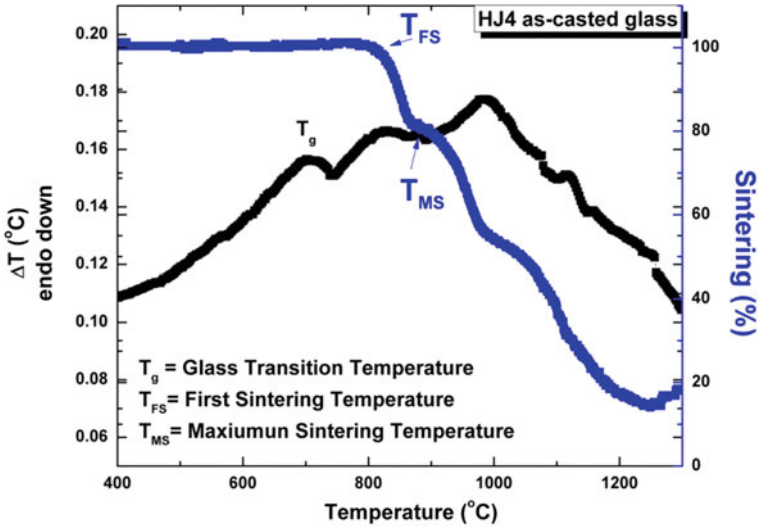

Fig. 11 DTA and HSM analysis of HJ4 as-cast glass; the analysis was performed at a heating rate of 5 °C/min [48]

during the DTA analysis. The corresponding HSM curve shows that the sintering process starts at (T_{FS}) 809 °C, while complete sintering was obtained at (T_{MS}) 875 °C followed by continuous viscous flow. To achieve a dense and leakage-free sealant, it is necessary to complete the sintering before the start of crystallization, thus avoiding the formation of porosity in the glass–ceramic due to increased viscosity triggered by crystal growth [3, 6]. From the DTA and HSM analyses, it is clear that the sintering process was completed at 875 °C and no evidence of crystallization was detected by DTA, thus ensuring the formation of a dense sealant. Moreover, the presence of a low degree of crystallization (higher residual glass) further promoted the formation of a dense sealant due to the viscous flow above the glass transition temperature.

From the data obtained from DTA and HSM, a heat treatment of 950 °C with a dwelling time of 5 h at a heating rate of 2 °C/min was used to process an optimal joining treatment. The as-joined HJ4 glass–ceramic showed a CTE of 9.3 10^{-6} K^{-1} which is a value within the desired range (9–12 × 10^{-6} K^{-1}), taking into consideration the CTEs of the other cell components (CTEs for Crofer22APU and 3YSZ are 12 × 10^{-6} K^{-1} and 10.5 × 10^{-6} K^{-1} respectively) [24, 49]. Further details about the crystalline phases that were observed are discussed in the later sections of this chapter.

A SEM cross-section of the HJ4 glass–ceramic in contact with Crofer22APU and 3YSZ substrates is shown in Fig. 12. The joining area was found to be crack-free with no evidence of delamination at the two interfaces, thus indicating very good thermomechanical compatibility. The microstructure is dense with a negligible concentration of closed pores. Various crystals are uniformly distributed into the residual glassy phase as shown in the magnified image (Fig. 12). The EDS point analysis carried out at different areas of the HJ4 as-joined glass–ceramic is shown

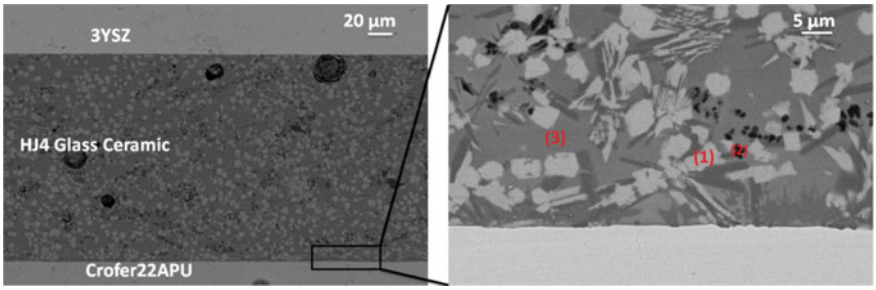

Fig. 12 SEM cross-section of Crofer22APU/HJ4 glass–ceramic/3YSZ joined sample [48]

Table 2 EDS point analysis (at.%) carried out on HJ4 as-joined glass–ceramic, shown in Fig. 12 [48]

Elements	Point 1	Point 2	Point 3
O	68.6	74.3	72.4
Si	15.6	16.4	15.8
Sr	14.9	5.5	8.2
Al	0.4	3.8	2.2
Y	0.5	0.0	1.4

in Table 2. The EDS analysis at the bright crystals (point 1) shows a phase based on silicon, strontium and oxygen and from the EDS composition, this was identified to be $SrSiO_3$, while the black crystals (point 2) represent a silica-rich phase. The EDS point analysis conducted at the residual glassy phase (point 3) is also shown in Table 2; the presence of 8.2 at.% Sr is beneficial to have good wettability of residual glassy phase.

The XRD patterns of the as-joined HJ4 glass–ceramics as well as after ageing are shown in Fig. 13. The XRD analysis confirmed the presence of $SrSiO_3$ as the main crystalline phase, in addition to SiO_2 (cristobalite) as the secondary phase. The XRD pattern for the HJ4 glass–ceramic after ageing at 850 °C for 1000 h is also shown in Fig. 13. The identical patterns after joining and ageing indicates that the HJ4 glass–ceramic is stable and no new phase formation was detected after ageing.

The SEM and XRD analysis have confirmed that a suitable SiO_2/SrO ratio has resulted in the formation of the high CTE $SrSiO_3$ phase. However, a SiO_2/SrO of ~ 2 also resulted in the formation of cristobalite phase. Due to phase transformation and consequently volume change, in cristobalite around 270 °C [50], its presence might determine thermomechanical stresses with possible crack formation, thus affecting the reliability of sealant during thermal cycles.

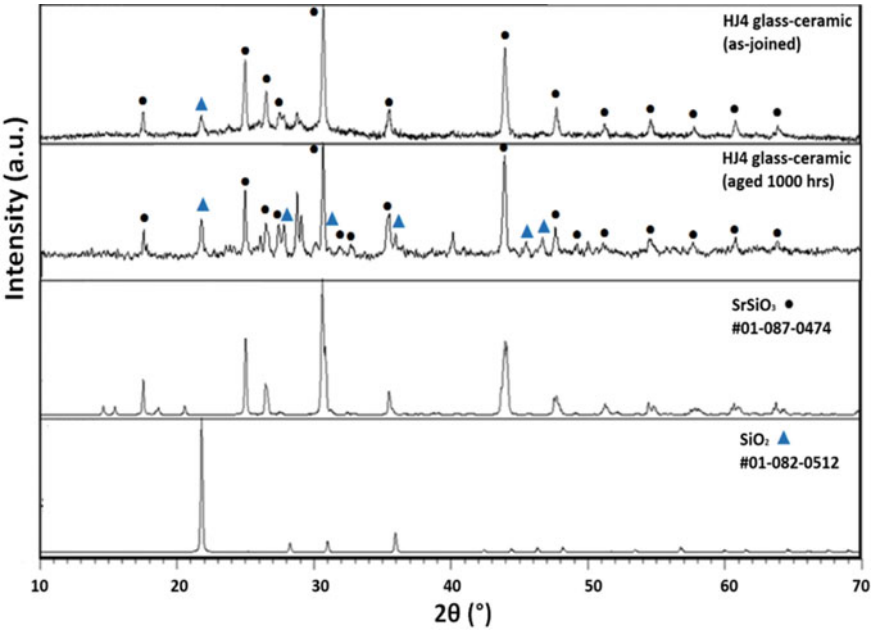

Fig. 13 XRD analysis of as-joined and thermally aged (1000 h, 850 °C) HJ4 glass–ceramic [48]

1.2.2 Electrical Properties and Post-Mortem Analysis

For SOC applications, the sealants should have high resistivity in order to avoid electrical short circuit. For long-term operation, any possible microstructural changes of the sealing glasses must be considered. This is of particular importance especially considering that interfacial reactions with the interconnect may be boosted by an applied voltage. To analyse and address this issue, the electrical resistivity of Crofer/HJ4 glass–ceramic/Crofer joined samples was measured at 850 °C under an applied voltage of 1.6 V. Figure 14 shows a schematic diagram of the test as well as the corresponding electrical resistivity curve of the joined sample. The resistivity is in the range of (10^6–10^7 Ω cm) and is higher than the minimum value (10^4 Ω cm) required to ensure electrical insulation and to work effectively in the SOC working conditions. Moreover, the electrical resistivity of HJ4 glass–ceramic is similar or slightly higher than the resistivity values reported in literature [15, 32, 51].

Figure 14 shows that after an initial reduction in the electrical resistivity during the first 200 h of testing, a constant resistivity was measured until 800 h. The continuous reduction at start of resistivity analysis is due to the fact that the as-joined HJ4 glass–ceramic has significantly high level of residual glass, where the presence of different free ions (such as Si, Sr, O, Sr, Al) can move under applied voltage and can cause reduction in resistivity. Around 800 h, another discontinuity caused further reduction in electrical resistivity. This second discontinuity is most likely due to polarization

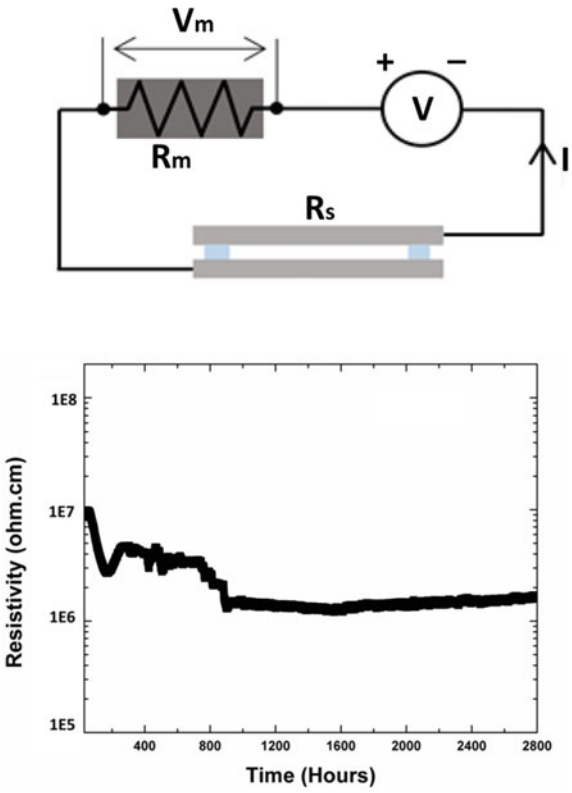

Fig. 14 Electrical resistivity of Crofer22APU/glass–ceramics/Crofer22APU joined samples for HJ4 glass–ceramics. These measurements were carried out at 850 °C with 1.6 V applied [52]

effects. Nevertheless, after 800 h the resistivity values for the HJ4-based joint became constant and no abnormalities or gaps were observed until the end of test.

After the electrical resistivity analysis, SEM–EDS post-mortem analyses were carried out to investigate the compatibility of the HJ4 glass–ceramic with an anodic polarized Crofer22APU plate and the results are shown in Fig. 15. The microstructure of the HJ4 glass–ceramic is homogenous, dense with apparently no signs of porosity, showing a good adhesion and an excellent compatibility with the Crofer22APU substrate. The microstructure is similar to that of as-joined glass–ceramic where a bright crystalline phase of $SrSiO_3$ is distributed within the residual amorphous matrix together with the presence of black cristobalite (SiO_2) crystals. Although a thin (~ 2 μm) MnCr-rich oxide scale is present at the interface, Cr is confined within the oxide scale without any diffusion into the glass–ceramic. Nevertheless, some traces of Mn diffusion into the residual glass are observed. Anyway, no further elements diffused or segregate from the glass–ceramic and the Crofer22APU. These results demonstrated that HJ4 glass–ceramic is chemically stable after long-term ageing at high temperature and under electric load.

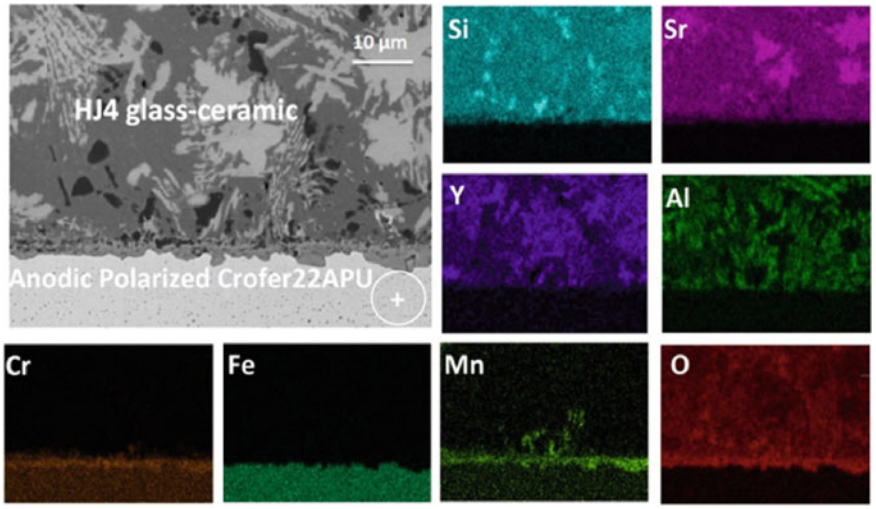

Fig. 15 EDS mapping of the SEM image corresponding to the post mortem analyses of anodic polarized Crofer22APU/HJ4 glass–ceramic interface, after the electrical resistivity test for 2800 h in static air, under a voltage of 1.6 V [52]

The formation of $SrCrO_4$ has frequently been observed in Sr-containing glasses and can harmfully affect the compatibility of sealants with Cr-based metallic interconnects due to its high CTE (18–20 $\times$ 10^{-6} K^{-1}) [53, 54]. However, despite the presence of a Cr-rich oxide scale, the Crofer22APU/sealant interface did not show any indication of the $SrCrO_4$ phase, thus maintaining an excellent adhesion.

The cathodic Crofer22APU/sealant interface also showed no segregation of elements from the glass–ceramic. The EDS mapping (Fig. 16) detected a small concentration of Cr and Mn that has been diffused from the Crofer22APU to the sealant. Sabato et al. [14] reported similar data, and observed outward diffusion of Cr and Mn close to the cathodic polarized interface. The results reported by Sabato et al. [14] after 100 h of testing, showed that around 4 at.% Cr was detected at approx. 10 µm from the interface. However, the diffusion in case of HJ4 glass–ceramic is limited, likely due to a slight lower amount of residual glassy phase. Finally, no interaction or signs of formation of the $SrCrO_4$ phase were found from SEM–EDS analyses, thus demonstrating an excellent compatibility with the Crofer22APU substrate.

1.2.3 Mechanical Properties and Post Mortem Analysis

Reliable operation of SOC devices can be critically determined on the mechanical behaviour of the sealants when in contact with the metallic interconnect. Mechanical issues can have a key impact on the performance and degradation rate of the SOFC/SOEC device and there is a relatively small body of literature that is concerned

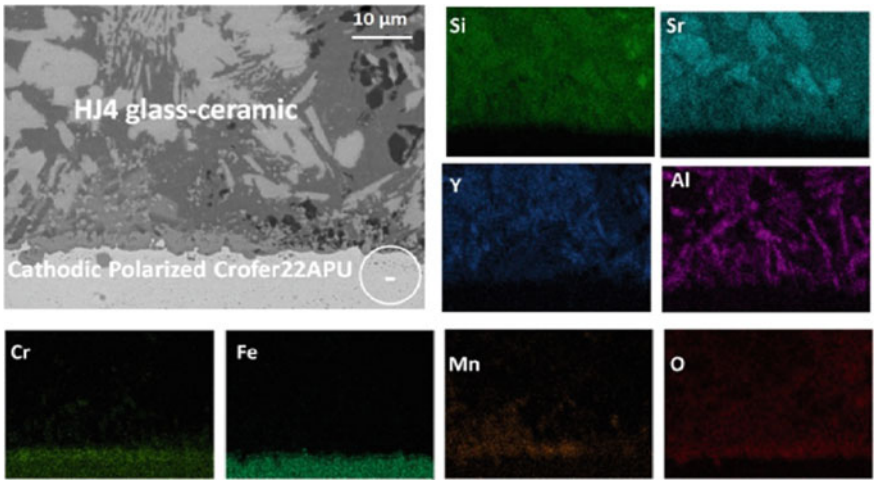

Fig. 16 EDS mapping of SEM image corresponding to post mortem analyses of cathodic polarized Crofer22APU/HJ4 glass–ceramic interface, after the electrical resistivity test for 2800 h in static air, under a voltage of 1.6 V [52]

with the mechanical properties of sealants both at RT and at operating conditions [8, 32–36, 55–58].

In order to evaluate the mechanical stability and shear resistance of the sealant, Crofer22APU/HJ4 glass–ceramic/Crofer22APU joints were prepared to investigate their behaviour under shear load conditions. The mechanical stability and shear strength of joined samples were measured at room temperature, 650 °C (below T_g) and at 850 °C (working temperature of SOC). Figure 17 illustrates the sample configuration (including dimensions) and setup used for mechanical testing of the joined samples under the shear load.

Figure 18a shows the shear stress versus load displacement data for the HJ4 joint samples, tested at RT, 650 °C and 850 °C respectively. It is worth mentioning that the slope of the plot can be slightly different due to possible inexact value of the joint area that was measured during the post mortem analysis of the fractured surfaces. The stress versus load curves show the effect of the test temperature on the resulting shear stress. When the Crofer22APU/HJ4 glass–ceramic/Crofer22APU joined samples were tested below T_g (at RT and at 650 °C), the stress versus displacement curve reflects almost linear elastic deformation until fracture and a brittle behaviour of the glass–ceramic joint. On the other hand, for shear testing performed at 850 °C ($T > T_g$), an enhanced displacement was observed for Crofer22APU/HJ4 glass–ceramic/Crofer22APU joint under applied shear load. This effect was as expected and is due to the softening of the residual glassy phase above T_g, that resulted in glass viscous flow. The softening of HJ4 glass–ceramic sealant at 850 °C can promote the stress relaxation phenomenon that can reduce thermal stresses at high temperature. Besides that, viscous flow of the residual glassy phase can lead to self-healing and improved long-term integrity of the sealant. Such stress relaxation phenomenon is

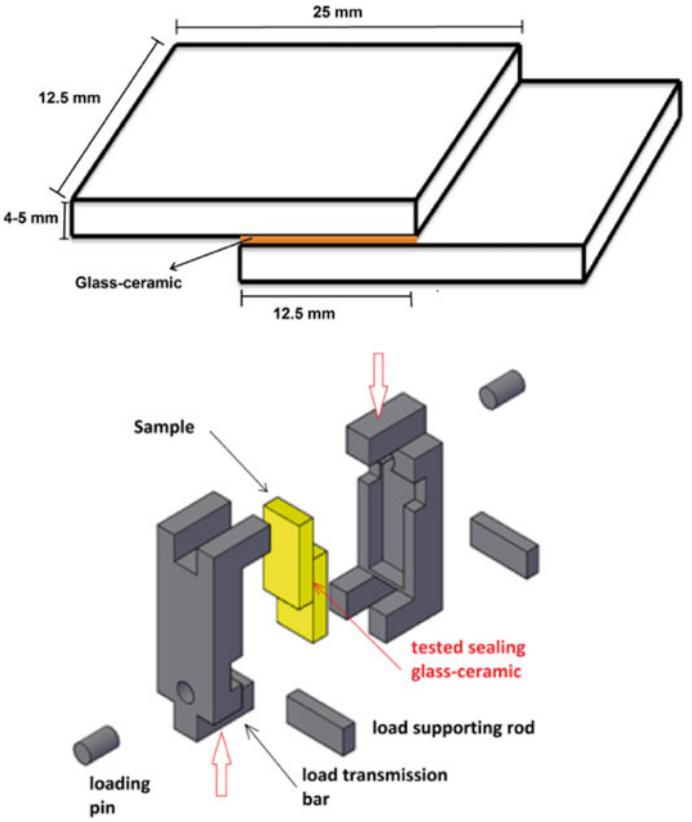

Fig. 17 Illustration of Crofer22APU/glass–ceramic/Crofer22APU samples with glass ceramic joint for shear testing (left) and setup for testing the sample under shear load (right) [59]

also reported in literature. For instance, according to Chang et al. [60], the viscoelastic behaviour of the residual glassy phase in GC-9 glass–ceramic system showed the stress relaxation at the temperature range of 650–750 °C.

The shear strength of the joined samples as calculated from the stress displacement curves are given in Fig. 18b. The average shear strength obtained after testing three samples at each test temperature is shown in Fig. 18b. The shear strength of the joined samples was reduced with the increase in the testing temperatures i.e., the shear strength of 13.9 MPa was measured at RT, however, testing at 850 °C showed shear strength of 1.8 MPa. As mentioned earlier, the residual glassy phase becomes viscous above T_g, therefore, the observed reduction in the strength with increasing temperature was due to the viscous flow occurring at the softening of the glassy phase at high temperature.

Figure 18c shows the elastic modulus of the HJ4 glass–ceramic measured by vibrational method from room temperature to 650 °C. The measurements were performed both during the heating and cooling stages as shown in Fig. 18c The elastic modulus

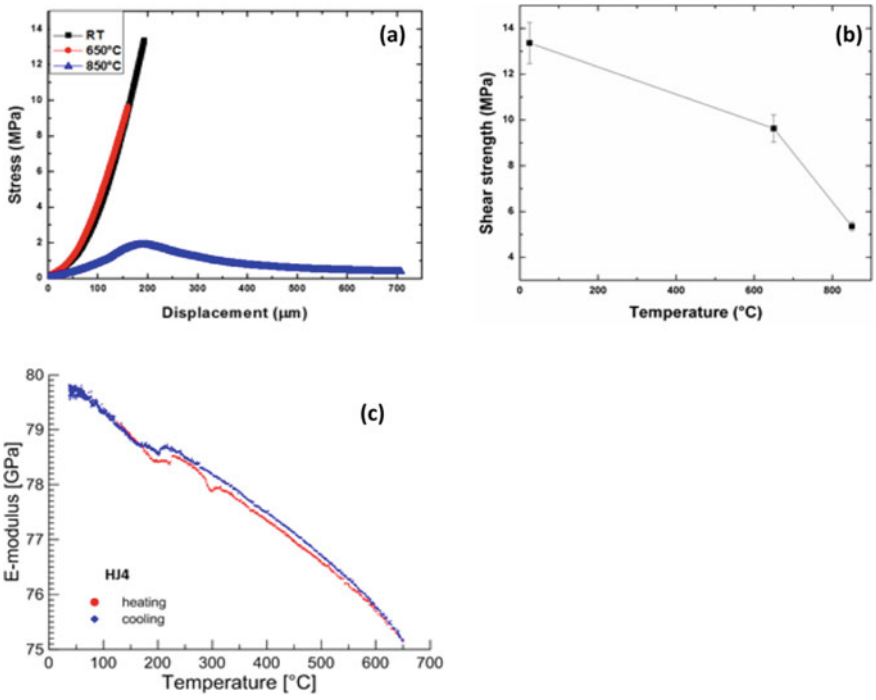

Fig. 18 **a** Shear stress versus displacement curves for HJ4 joints, **b** shear strength versus temperature for HJ4 joints, and **c** elastic modulus of HJ4 glass–ceramic [59]

curves for the HJ4 glass–ceramic during heating and cooling show overlapping, thus indicating that no microstructural changes occurred within the glass–ceramic. On the other hand, some discontinuities are visible in Fig. 18c around 230 °C during the heating cycle and around 230–270 °C during cooling. These are due to the presence of the cristobalite (SiO_2) phase in the HJ4 glass–ceramic that shows volume expansion around 230–270 °C. Nevertheless, the obtained elastic modulus value is comparable with measurements reported in the literature (50–80 GPa) [39, 62].

In order to better understand the mechanical behaviour as described above, it is important to investigate the fracture surfaces as well as cross-sections of samples after fracture. Figure 19 shows the SEM cross section images of the Crofer22APU/HJ4 glass–ceramic fractured interfaces. The SEM images showed a uniform microstructure of glass and strong bonding with the Crofer22APU at room temperature as well as at higher testing temperatures, with no evidence of any crack or delamination. The Crofer22APU/HJ4 glass–ceramic interface showed comparable morphology. The HJ4 glass–ceramic microstructure after mechanical testing at different temperatures is also similar to the as-joined HJ4 glass–ceramic as shown in Fig. 12.

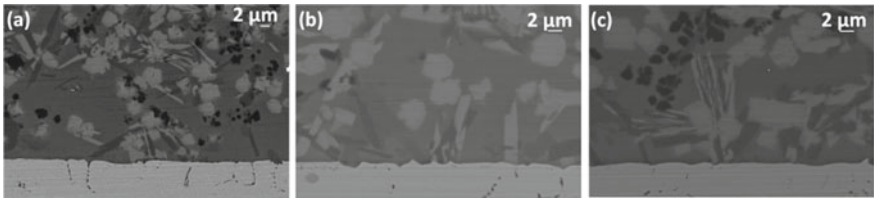

Fig. 19 SEM images of interface of Crofer22APU with **a** HJ4 tested at RT, **b** HJ4 tested at 650 °C, **c** HJ4 tested at 850 °C [59]

2 Conclusions

The purpose of the current chapter was to present and discuss different approaches in the design and specific tests of glass-based materials as sealants for SOCs.

One of the more significant findings to emerge from this comparison is that a single and ideal sealant does not exists, since the performances are strictly related to the SOC design and the operating conditions.

The findings of this study suggest that Na-containing glass sealants suffer from the concurrent high voltage application and contact with chromia forming alloys.

The current data highlight the importance of protective coatings needed to overcome this issue.

Main results on research activity done in the past 10 years at the Politecnico di Torino on both Na-and Sr-containing sealants have been presented and discussed for SOC applications in the T range 750–850 °C. Different glass compositions have been designed and successfully tested, thus providing a deeper insight into relationships between glass compositions, characteristic temperature and SOC operating conditions.

The right balance of sealants composition plays a key role in obtaining the desired high-CTE phases in the glass–ceramic and a dense sealant with sufficient quantity of the residual glassy phase that is beneficial for stress relaxation below T_g.

The detailed studies conducted at Politecnico di Torino, Italy, showed that both Na and Sr-based glass–ceramics can be promising candidates to use for SOC sealant applications.

Bibliography

1. Holland, W., Beall, G.: Glass-Ceramic Technology. The American Ceramic Society, Westerville (2002)
2. Donald, I.W., Mallinson, P.M., Metcalfe, B.L., Gerrard, L.A., Fernie, J.A.: Recent developments in the preparation, characterization and applications of glass-and glass–ceramic-to-metal seals and coatings. J. Mater. Sci. **46**, 1975–2000 (2011). https://doi.org/10.1007/s10853-010-5095-y
3. Mahapatra, M.K., Lu, K.: Seal glass for solid oxide fuel cells. J. Power Sources **195**, 7129–7139 (2010). https://doi.org/10.1016/j.jpowsour.2010.06.003

4. Schilm, J., Rost, A., Poenicke, A., Kusnezoff, M., Michaelis, A.: Ceramic integration technologies for solid oxide fuel cells. Int. J. Appl. Ceram. Technol. **9**, 688–699 (2012). https://doi.org/10.1111/j.1744-7402.2012.02789.x
5. Mahapatra, M.K., Lu, K.: Glass-based seals for solid oxide fuel and electrolyzer cells—a review. Mater. Sci. Eng. R Reports. **67**, 65–85 (2010). https://doi.org/10.1016/j.mser.2009.12.002
6. Fergus, J.W.: Sealants for solid oxide fuel cells. J. Power Sources **147**, 46–57 (2005). https://doi.org/10.1016/j.jpowsour.2005.05.002
7. Chou, Y.S., Stevenson, J.W., Choi, J.P.: Long-term evaluation of solid oxide fuel cell candidate materials in a 3-cell generic short stack fixture, part II: sealing glass stability, microstructure and interfacial reactions. J. Power Sources **250**, 166–173 (2014). https://doi.org/10.1016/j.jpowsour.2013.09.148
8. Ritucci, I., Kiebach, R., Talic, B., et al.: Improving the interface adherence at sealings in solid oxide cell stacks. J. Mater. Res. **34**, 1167–1178 (2019). https://doi.org/10.1557/jmr.2018.459
9. Gödeke, D., Dahlmann, U.: Study on the crystallization behaviour and thermal stability of glass-ceramics used as solid oxide fuel cell-sealing materials. J. Power Sources **196**, 9046–9050 (2011). https://doi.org/10.1016/j.jpowsour.2010.12.054
10. Smeacetto, F., Salvo, M., Ferraris, M., Cho, J., Boccaccini, A.R.: Glass–ceramic seal to join Crofer 22 APU alloy to YSZ ceramic in planar SOFCs. J. Eur. Ceram. Soc. **28**, 61–68 (2008). https://doi.org/10.1016/j.jeurceramsoc.2007.05.006
11. Sabato, A.G., Salvo, M., De Miranda, A., Smeacetto, F.: Crystallization behaviour of glass–ceramic sealant for solid oxide fuel cells. Mater. Lett. **141**, 284–287 (2015). https://doi.org/10.1016/j.matlet.2014.11.128
12. Smeacetto, F., De Miranda, A., Chrysanthou, A., Bernardo, E., Secco, M., Bindi, M., Salvo, M., Sabato, A.G., Ferraris, M.: Novel glass-ceramic composition as sealant for SOFCs. J. Am. Ceram. Soc. **97**, 3835–3842 (2014). https://doi.org/10.1111/jace.13219
13. Sabato, A.G., Cempura, G., Montinaro, D., Chrysanthou, A., Salvo, M., Bernardo, E., Secco, M., Smeacetto, F.: Glass–ceramic sealant for solid oxide fuel cells application: characterization and performance in dual atmosphere. J. Power Sources **328**, 262–270 (2016). https://doi.org/10.1016/j.jpowsour.2016.08.010
14. Sabato, A.G., Rost, A., Schilm, J., Kusnezoff, M., Salvo, M., Chrysanthou, A., Smeacetto, F.: Effect of electric load and dual atmosphere on the properties of an alkali containing diopside-based glass sealant for solid oxide cells. J. Power Sources **415** (2019). https://doi.org/10.1016/j.jpowsour.2019.01.051
15. Chou, Y.S., Stevenson, J.W., Xia, G.G., Yang, Z.G.: Electrical stability of a novel sealing glass with (Mn, Co)-spinel coated Crofer22APU in a simulated SOFC dual environment. J. Power Sources **195**, 5666–5673 (2010). https://doi.org/10.1016/j.jpowsour.2010.03.052
16. Smeacetto, F., De Miranda, A., Sandra Cabanas Polo, S.M., Boccaccini, D., Salvo, M., Boccaccini, A.R.: Electrophoretic deposition of $Mn_{1.5}Co_{1.5}O_4$ on metallic interconnect and interaction with glass–ceramic sealant for solid oxide fuel cells application. J. Power Sources **280**, 379–386 (2015). https://doi.org/10.1016/j.ijhydene.2013.04.106
17. Smeacetto, F., De Miranda, A., Cabanas Polo, S., Molin, S., Boccaccini, D., Salvo, M., Boccaccini, A.R.: Electrophoretic deposition of $Mn_{1.5}Co_{1.5}O_4$ on metallic interconnect and interaction with glass–ceramic sealant for solid oxide fuel cells application, J. Power Sources **280**, 379–386 (2015). https://doi.org/10.1016/j.jpowsour.2015.01.120
18. Smeacetto, F., Salvo, M., Leone, P., Santarelli, M., Ferraris, M.: Performance and testing of joined Crofer22APU-glass–ceramic sealant-anode supported cell in SOFC relevant conditions. Mater. Lett. **65**, 1048–1052 (2011). https://doi.org/10.1016/j.matlet.2010.12.050
19. Ogasawara, K., Kameda, H., Matsuzaki, Y., Sakurai, T.: Chemical stability of ferritic alloy interconnect for SOFCs. J. Electrochem. Soc. **154**, B657–B663 (2007). https://doi.org/10.1149/1.2735919
20. Coillot, D., Me, O.: New viscous sealing glasses for electrochemical cells. Int. J. Hydrogen Energy **37**, 9351–9358 (2012). https://doi.org/10.1016/j.ijhydene.2012.02.194
21. Shyam, A., Trejo, R., McClurg, D., Ladouceur, A., Kirkham, M., Song, X., Howe, J., Lara-Curzio, E.: Microstructural evolution in two alkali multicomponent silicate glasses as a result of

long-term exposure to solid oxide fuel cell environments. J. Mater. Sci. **48**, 5880–5898 (2013). https://doi.org/10.1007/s10853-013-7384-8
22. Smeacetto, F., Salvo, M., Ferraris, M., Casalegno, V., Asinari, P.: Glass and composite seals for the joining of YSZ to metallic interconnect in solid oxide fuel cells. J. Eur. Ceram. Soc. **28**, 611–616 (2008). https://doi.org/10.1016/j.jeurceramsoc.2007.07.008
23. Smeacetto, F., Chrysanthou, A., Salvo, M., Moskalewicz, T., D'Herin Bytner, F., Ajitdoss, L.C., Ferraris, M.: Thermal cycling and ageing of a glass-ceramic sealant for planar SOFCs. Int. J. Hydrogen Energy **36,** 11895–11903 (2011). https://doi.org/10.1016/j.ijhydene.2011.04.083
24. Mah, J.C.W., Muchtar, A., Somalu, M.R., Ghazali, M.J.: Metallic interconnects for solid oxide fuel cell: a review on protective coating and deposition techniques, Int. J. Hydrogen Energy pp. 1–11 (2015). https://doi.org/10.1016/j.ijhydene.2016.03.195
25. Shaigan, N., Qu, W., Ivey, D.G., Chen, W.: A review of recent progress in coatings, surface modifications and alloy developments for solid oxide fuel cell ferritic stainless steel interconnects. J. Power Sources **195**, 1529–1542 (2010). https://doi.org/10.1016/j.jpowsour.2009.09.069
26. Zanchi, E., Sabato, A.G., Molin, S., Cempura, G., Boccaccini, A.R., Smeacetto, F.: Recent advances on spinel-based protective coatings for solid oxide cell metallic interconnects produced by electrophoretic deposition. Mater. Lett. **286**, 129229 (2021). https://doi.org/10.1016/j.matlet.2020.129229
27. Ritucci, I., Agersted, K., Zielke, P., Wulff, A.C., Khajavi, P., Smeacetto, F., Sabato, A.G., Kiebach, R.: A Ba-free sealing glass with a high coefficient of thermal expansion and excellent interface stability optimized for SOFC/SOEC stack applications. Int. J. Appl. Ceram. Technol. **15**, 1011–1022 (2018). https://doi.org/10.1111/ijac.12853
28. Qi, H.B., Lees, D.G.: The effects of surface-applied oxide films containing varying amounts of yttria, chromia, or alumina on the high-temperature oxidation behavior of chromia-forming and alumina-forming alloys. Oxid. Met. **53**, 507–527 (2000). https://doi.org/10.1023/A:1004633026323
29. Chou, Y.S., Choi, J.P., Stevenson, J.W.: Compliant alkali silicate sealing glass for solid oxide fuel cell applications: the effect of protective alumina coating on electrical stability in dual environment. Int. J. Hydrogen Energy **37**, 18372–18380 (2012). https://doi.org/10.1016/j.ijhydene.2012.08.084
30. Chou, Y., Thomsen, E.C., Choi, J., Stevenson, J.W.: Compliant alkali silicate sealing glass for solid oxide fuel cell applications: the effect of protective YSZ coating on electrical stability in dual environment. J. Power Sources **202**, 149–156 (2012). https://doi.org/10.1016/j.jpowsour.2011.11.017
31. Sabato, A.G., Chrysanthou, A., Salvo, M., Cempura, G., Smeacetto, F.: Interface stability between bare, Mn–Co spinel coated AISI 441 stainless steel and a diopside-based glass–ceramic sealant. Int. J. Hydrogen Energy **43**, 1824–1834 (2018). https://doi.org/10.1016/j.ijhydene.2017.11.150
32. Chou, Y.-S.S., Stevenson, J.W., Choi, J.-P.: Alkali effect on the electrical stability of a solid oxide fuel cell sealing glass. J. Electrochem. Soc. **157**, B348–B353 (2010). https://doi.org/10.1111/j.1551-2916.2009.03466.x
33. Reddy, A.A., Tulyaganov, D.U., Goel, A., Pascual, M.J., Kharton, V.V., Tsipis, E.V., Ferreira, J.M.F.: Diopside-Mg orthosilicate and diopside-Ba disilicate glass-ceramics for sealing applications in SOFC: sintering and chemical interactions studies. Int. J. Hydrogen Energy **37**, 12528–12539 (2012). https://doi.org/10.1016/j.ijhydene.2012.05.130
34. Yang, Z., Meinhardt, K.D., Stevenson, J.W.: Chemical compatibility of barium–calcium–aluminosilicate-based sealing glasses with the ferritic stainless steel interconnect in SOFCs. J. Electrochem. Soc. **150**, A1095 (2003). https://doi.org/10.1149/1.1590325
35. Javed, H., Sabato, A.G., Mansourkiaei, M., Ferrero, D., Santarelli, M., Herbrig, K., Walter, C., Smeacetto, F.: Glass–ceramic sealants for SOEC: thermal characterization and electrical resistivity in dual atmosphere. Energies **13**, 3682 (2020). https://doi.org/10.3390/en13143682
36. Ferraris, M., De la Pierre, S., Sabato, A.G., Smeacetto, F., Javed, H., Walter, C., Malzbender, J.: Torsional shear strength behavior of advanced glass–ceramic sealants for SOFC/SOEC

applications. J. Eur. Ceram. Soc. **40**, 4067–4075 (2020). https://doi.org/10.1016/j.jeurceramsoc.2020.04.034
37. Kothiyal, G.P., Goswami, M., Tiwari, B., Sharma, K., Ananthanarayanan, A., Montagne, L.: Some recent studies on glass/glass–ceramics for use as sealants with special emphasis for high temperature applications. J. Adv. Ceram. **1**, 110–129 (2012). https://doi.org/10.1007/s40145-012-0009-x
38. Kaur, M., Kaur, G., Pandey, O.P., Singh, K., Kumar, V.: Influence of CaO/MgO ratio on the crystallization kinetics and interfacial compatibility with crofer 22APU and YSZ of strontium based alumino-borosilicate glasses for SOFC applications. Int. J. Hydrogen Energy **42**, 16244–16257 (2017). https://doi.org/10.1016/j.ijhydene.2017.05.026
39. Fakouri Hasanabadi, M., Faghihi-Sani, M.A., Kokabi, A.H., Groß-Barsnick, S.M., Malzbender, J.: Room-and high-temperature flexural strength of a stable solid oxide fuel/electrolysis cell sealing material. Ceram. Int. 1–7 (2018). https://doi.org/10.1016/j.ceramint.2018.09.236
40. Luo, Z., Lei, W., Liang, H., Xu, W., Liu, X., Qin, C., Lu, A.: Improving sealing properties of CaO–SrO–Al_2O_3–SiO_2 glass and glass–ceramics for solid oxide fuel cells: effect of La_2O_3 addition. Ceram. Int. **46**, 17698–17706 (2020). https://doi.org/10.1016/j.ceramint.2020.04.074
41. Wang, X., Ou, D.R., Zhao, Z., Cheng, M.: Stability of SrO–La_2O_3–Al_2O_3–SiO_2 glass sealants in high-temperature air and steam. Ceram. Int. **42**, 7514–7523 (2016). https://doi.org/10.1016/j.ceramint.2016.01.158
42. Mahapatra, M.K., Lu, K., Reynolds, W.T.: Thermophysical properties and devitrification of SrO-La_2O_3–Al_2O_3–B_2O_3–SiO_2-based glass sealant for solid oxide fuel/electrolyzer cells. J. Power Sources **179**, 106–112 (2008). https://doi.org/10.1016/j.jpowsour.2007.12.101
43. Zhang, Q., Yang, H., Zeng, F., Wang, S., Tang, D., Zhang, T.: Development of the CaO–SrO–ZrO_2–B_2O_3–SiO_2 sealing glasses for solid oxide fuel cell applications: structure. RSC Adv. **5**, 41772–41779 (2015). https://doi.org/10.1039/C5RA04781A
44. Ojha, P.K., Chongdar, T.K., Gokhale, N.M., Kulkarni, A.R.: Investigation of crystallization kinetic of SrO–La_2O_3–Al_2O_3–B_2O_3–SiO_2 glass and its suitability for SOFC sealant. Int. J. Hydrogen Energy **36**, 14996–15001 (2011). https://doi.org/10.1016/j.ijhydene.2010.12.120
45. Reddy, A.A., Goel, A., Tulyaganov, D.U., Sardo, M., Mafra, L., Pascual, M.J., Kharton, V.V., Tsipis, E.V., Kolotygin, V.A., Ferreira, J.M.F.: Thermal and mechanical stability of lanthanide-containing glass–ceramic sealants for solid oxide fuel cells. J. Mater. Chem. A **2**, 1834 (2014). https://doi.org/10.1039/c3ta13196c
46. Mahapatra, M.K., Lu, K.: Effect of atmosphere on interconnect-seal glass interaction for solid oxide fuel/electrolyzer cells. J. Am. Ceram. Soc. **94**, 875–885 (2011). https://doi.org/10.1111/j.1551-2916.2010.04020.x
47. Elsayed, H., Javed, H., Sabato, A.G., Smeacetto, F., Bernardo, E.: Novel glass-ceramic SOFC sealants from glass powders and a reactive silicone binder. J. Eur. Ceram. Soc. **38**, 4245–4251 (2018). https://doi.org/10.1016/j.jeurceramsoc.2018.05.024
48. Javed, H., Sabato, A.G., Herbrig, K., Ferrero, D., Walter, C., Salvo, M., Smeacetto, F.: Design and characterization of novel glass-ceramic sealants for solid oxide electrolysis cell (SOEC) applications. Int. J. Appl. Ceram. Technol. **15**, 999–1010 (2018). https://doi.org/10.1111/ijac.12889
49. Kaur, G.: Solid Oxide Fuel Cell Components: Seal Glass for Solid Oxide Fuel Cells (2006). https://doi.org/10.1007/s11837-006-0052-6
50. Beals, M.D., Zerfoss, S.: Volume change attending low-to-high inversion of cristobalite. J. Am. Ceram. Soc. **27**, 285–292 (1944). https://doi.org/10.1111/j.1151-2916.1944.tb14471.x
51. Ghosh, S., Das Sharma, A., Kundu, P., Basu, R.N.: Glass-ceramic sealants for planar IT-SOFC: a bilayered approach for joining electrolyte and metallic interconnect. J. Electrochem. Soc. **155**, B473–B478 (2008). https://doi.org/10.1149/1.2883732
52. Javed, H., Herbrig, K., Sabato, A.G., Ferrero, D., Santarelli, M., Walter, C., Smeacetto, F.: Electrical characterization of glass-ceramic sealant-metallic interconnect joined samples under solid oxide electrolysis cell conditions; influence on the microstructure and composition at the different polarized interfaces. Ceram. Int. (2020). https://doi.org/10.1016/j.ceramint.2020.11.176

53. Chou, Y.S., Stevenson, J.W., Singh, P.: Effect of pre-oxidation and environmental aging on the seal strength of a novel high-temperature solid oxide fuel cell (SOFC) sealing glass with metallic interconnect. J. Power Sources **184**, 238–244 (2008). https://doi.org/10.1016/j.jpowsour.2008.06.020
54. Zhang, Q., Du, X., Tan, S., Tang, D., Chen, K., Zhang, T.: Effect of Nb_2O5 Doping on Improving the Thermo-mechanical Stability of Sealing Interfaces for Solid Oxide Fuel Cells, pp. 1–8 (2017). https://doi.org/10.1038/s41598-017-05725-y
55. Lin, C.K., Liu, Y.A., Wu, S.H., Liu, C.K., Lee, R.Y.: Joint strength of a solid oxide fuel cell glass–ceramic sealant with metallic interconnect in a reducing environment. J. Power Sources **280**, 272–288 (2015). https://doi.org/10.1016/j.jpowsour.2015.01.126
56. Fakouri Hasanabadi, M., Faghihi-Sani, M.A., Kokabi, A.H., Malzbender, J.: The analysis of torsional shear strength test of sealants for solid oxide fuel cells. Ceram. Int. **43**, 12546–12550 (2017). https://doi.org/10.1016/j.ceramint.2017.06.128
57. Smeacetto, F., De Miranda, A., Ventrella, A., Salvo, M., Ferraris, M.: Shear strength tests of glass ceramic sealant for solid oxide fuel cells applications. Adv. Appl. Ceram. **114**, S70–S75 (2015). https://doi.org/10.1179/1743676115Y.0000000042
58. Osipova, T., Wei, J., Pecanac, G., Malzbender, J.: Room and elevated temperature shear strength of sealants for solid oxide fuel cells. Ceram. Int. **42**, 12932–12936 (2016). https://doi.org/10.1016/j.ceramint.2016.05.064
59. Javed, H., Sabato, A.G., Dlouhy, I., Halasova, M., Bernardo, E., Salvo, M., Herbrig, K., Walter, C., Smeacetto, F.: Shear performance at room and high temperatures of glass–ceramic sealants for solid oxide electrolysis cell technology. Mater. **12**, 298 (2019). https://doi.org/10.3390/ma12020298
60. Chang, H.T., Lin, C.K., Liu, C.K.: Effects of crystallization on the high-temperature mechanical properties of a glass sealant for solid oxide fuel cell. J. Power Sources **195**, 3159–3165 (2010). https://doi.org/10.1016/j.jpowsour.2009.12.008
61. Zhao, Y., Malzbender, J., Gross, S.M.: The effect of room temperature and high temperature exposure on the elastic modulus, hardness and fracture toughness of glass ceramic sealants for solid oxide fuel cells. J. Eur. Ceram. Soc. **31**, 541–548 (2011). https://doi.org/10.1016/j.jeurceramsoc.2010.10.032
62. Wei, J., Osipova, T., Malzbender, J., Krüger, M.: Mechanical characterization of SOFC/SOEC cells. Ceram. Int. (2018). https://doi.org/10.1016/j.ceramint.2018.03.103